STUDIA UBB CHEMIA, LXX, 2, 2025 (p. 19-36)
(RECOMMENDED CITATION)
DOI:10.24193/subbchem.2025.2.02

KINETIC MODELING APPROACH TO *IN VIVO* INTERACTIONS OF CURCUMIN AND CURCUMINOID-PIPERINE MIXTURE WITH QUETIAPINE

Iulia Maria CIOCOTIȘAN[a], Dana Maria MUNTEAN[a]*, Laurian VLASE[a]

ABSTRACT. This study aimed to develop kinetic models that describe the preclinical drug interaction data between quetiapine, an atypical antipsychotic, and bioactive compounds derived from turmeric rhizome. The potential risk of interaction between these substances could alter the disposition of quetiapine and impact its efficacy. During the development of the kinetic models, first-order kinetic processes were assumed, and several hypotheses were evaluated, including the number of compartments for distribution, the presence of lag time in quetiapine absorption, the presystemic formation of its metabolite, and the relative bioavailability between the study groups. The most accurate models suggest that interactions between quetiapine and curcumin occur primarily at the intestinal level, as the systemic metabolism constant remained unaltered. Conversely, coadministration with curcuminoids and piperine markedly affected systemic metabolism, likely due to hepatic enzyme inhibition, resulting in a 59.6% increase in the relative bioavailability of quetiapine. The developed models successfully integrated data for quetiapine and norquetiapine, both as standalone administration and in combination with curcumin or curcuminoid-piperine bioactive compounds, capturing their disposition within the framework of pharmacokinetic interactions.

Keywords: *kinetic modeling, quetiapine, norquetiapine, curcumin, curcuminoids, drug interactions*

[a] *Department of Pharmaceutical Technology and Biopharmacy, Iuliu Haţieganu University of Medicine and Pharmacy, Cluj-Napoca, Romania*
[*] *Corresponding author: dana.muntean@umfcluj.ro*

INTRODUCTION

Quetiapine (QUE), a dibenzothiazepine derivative is employed in treating psychotic disorders [1], primarily due to its moderate antagonism towards serotonin $5HT_{2A}$, H_1 histamine and α_1 adrenergic receptors, alongside its low affinity for dopamine D2 receptors [2]. Immediate-release formulations exhibit rapid oral (p.o.) absorption, with a median time of 1–2 hours to reach maximum plasma concentration. QUE's moderate lipophilicity underpins its extensive volume of distribution (Vd) of 510–710 L and 83% plasma protein binding [2]. Metabolism predominantly occurs in the liver, with less than 1% excreted unchanged in urine. Phase I reactions, including oxidation, hydroxylation, and N-/O-dealkylation, followed by phase II conjugation, represent key metabolic pathways [3]. The cytochrome P450 (CYP) system—primarily the CYP3A4 isoenzyme, with minor contributions from CYP3A5 and CYP2D6—mediates QUE's clearance [4]. Intestinal CYP3A4 metabolism, occurring in enterocytes, further influences QUE's bioavailability – defined as the fraction of the administered dose that reaches systemic circulation and becomes available for therapeutic effect. CYP3A4 also converts QUE to its active metabolite, N-desalkylquetiapine (norquetiapine, NQ), which contributes to the overall antidepressant activity via noradrenaline reuptake inhibition, partial serotonin 5-HT1A agonism, and presynaptic α2 adrenergic and serotonin 5-HT2C/5-HT7 receptor antagonism. NQ undergoes subsequent CYP2D6-mediated metabolism, with limited involvement from CYP3A4 [5].

Curcumin, the principal bioactive compound of turmeric rhizome (*Curcuma longa Linn.),* has a diferuloylmethane structure, as depicted in Scheme 1, and belongs to the polyphenolic curcuminoid group, alongside demethoxycurcumin and bisdemethoxycurcumin.

Supplements containing turmeric rhizome extracts are recognized for their antioxidant, anti-inflammatory, and neuroprotective properties. However, curcumin alone demonstrated low oral bioavailability due to poor absorption and rapid metabolism at both pre- and systemic circulation [6]. One method to enhance curcumin's bioavailability involves the addition of piperine, an alkaloid with N-acyl pyridine structure. Piperine inhibits the rapid metabolism, including glucuronidation and potentially CYP enzymes, while increasing the intestinal permeability resulting in increased intestinal absorption. Both curcumin and piperine possess inhibitory activity towards a series of CYP enzymes, including CYP3A4 and CYP2D6 [7].

Patients prescribed antipsychotics often undergo polypharmacy due to coadministration of medications targeting the same condition or comorbidities. Curcumin and curcumin-derived formulations, with their anti-inflammatory and pro-cognitive effects, may complement psychiatric treatments and are likely to

be used alongside QUE [8]. Given their pharmacokinetic (PK) properties and shared interaction with CYP enzymes, a PK interaction between QUE and curcuminoids is plausible. Assessing this interaction is essential to ensure therapeutic efficacy and safety during concomitant administration.

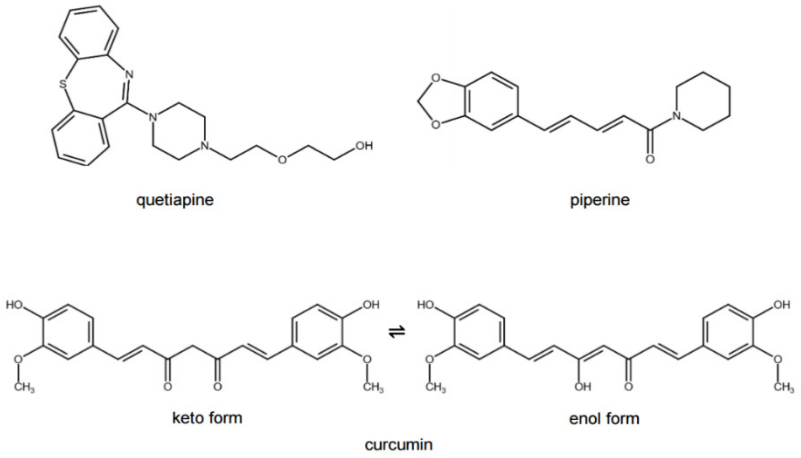

Scheme 1. Structural formulas of quetiapine, piperine and curcumin (keto form – bottom left, enol form – bottom right)

PK modeling utilizes mathematical approaches to describe the absorption, distribution, metabolism, and excretion (ADME) of drugs, enabling predictions of their behavior across various physiological conditions [9]. Compartmental modeling simplifies ADME processes by grouping tissues and fluids with similar characteristics into compartments. These virtual spaces approximate drug movement and enhance predictions of PK behaviour. PK models primarily focus on temporal changes in drug concentration or amount within the body. Key steps in developing such models include identifying the structural framework, defining the number of compartments, and estimating relevant PK parameters [10].

The aim of this study was to develop kinetic models that comprehensively describe the absorption, distribution, metabolism, and elimination processes of QUE and its metabolite NQ, following the administration of a single dose of QUE after previous treatment with either crude curcumin or a combination of curcuminoids and piperine. This was achieved by comparing predicted data with the experimental results obtained from an *in vivo* rat study.

RESULTS AND DISCUSSION

Table 1 and Table 2 present the mean plasma concentration-time profiles and the standard deviation (S.D.) for QUE and its active metabolite, NQ, across the three study groups, which were used for kinetic modeling.

Table 1. The mean ± S.D. plasma concentration-time values of quetiapine (85 mg/kg b.w., *p.o.*) single-dose across three study groups: quetiapine monotherapy (Reference, n=13), 6-day pre-treatment with curcumin (200 mg/kg b.w. *p.o.*, Test 1, n=13) and 6-day pre-treatment with curcuminoid (200 mg/kg b.w., *p.o.*)/piperine formulation (Test 2, n=13)

Time (h)	QUE Concentration (ng/mL)		
	Reference	Test 1	Test 2
0.16	126.7 ± 50.9	70.6 ± 47.7	74.5 ± 24.8
0.33	323.1 ± 187.3	121.6 ± 73.0	229.6 ± 82.4
0.5	383.7 ± 240.9	158.5 ± 96.7	316.4 ± 168.8
0.75	364.4 ± 297.7	192.3 ± 87.7	350.7 ± 158.9
1.0	349.8 ± 307.6	210.1 ± 88.0	439.2 ± 269.5
1.5	308.5 ± 194.3	227.1 ± 102.0	471.1 ± 311.3
2.0	272.3 ± 151.3	224.5 ± 122.9	482.2 ± 274.1
2.5	252.6 ± 148.5	215.5 ± 144.4	415.2 ± 236.4
3.0	226.0 ± 140.1	186.2 ± 110.0	364.6 ± 192.1
4.0	152.2 ± 90.7	155.1 ± 117.8	253.1 ± 122.1
6.0	76.4 ± 42.4	101.7 ± 77.1	153.2 ± 79.0
8.0	53.6 ± 38.5	50.5 ± 47.8	83.5 ± 44.0
10.0	39.0 ± 24.9	25.9 ± 22.4	63.7 ± 46.5
12.0	20.4 ± 12.9	19.5 ± 14.6	33.4 ± 18.4
16.0	9.9 ± 7.4	16.5 ± 10.9	26.0 ± 15.5
20.0	7.7 ± 4.5	12.2 ± 6.1	17.2 ± 7.7
24.0	6.3 ± 5.4	7.6 ± 4.3	14.2 ± 9.3
30.0	6.5 ± 3.9	4.5 ± 2.8	5.9 ± 2.9

Table 2. The mean ± S.D. plasma concentration-time values of norquetiapine across three study groups

Time (h)	NQ Concentration (ng/mL)		
	Reference	Test 1	Test 2
0.16	120.9 ± 69.8	149.7 ± 108.4	123.7 ± 54.8
0.33	192.9 ± 98.0	212.9 ± 130.4	219.8 ± 70.3
0.5	239.8 ± 97.9	262.1 ± 127.8	255.3 ± 86.8
0.75	237.1 ± 96.4	303.3 ± 156.0	297.5 ± 146.9
1.0	230.0 ± 69.6	338.1 ± 161.2	331.9 ± 177.9
1.5	229.1 ± 72.9	356.6 ± 169.2	358.1 ± 168.9
2.0	226.9 ± 71.5	358.7 ± 182.6	361.4 ± 173.4
2.5	224.4 ± 72.0	352.2 ± 175.9	330.3 ± 145.8
3.0	209.2 ± 65.6	343.0 ± 166.0	320.1 ± 146.4
4.0	178.8 ± 58.4	298.7 ± 166.6	289.1 ± 138.1
6.0	135.1 ± 52.2	234.4 ± 143.2	236.0 ± 130.1
8.0	102.8 ± 56.4	181.2 ± 150.9	177.2 ± 125.0
10.0	70.6 ± 55.6	116.0 ± 124.5	137.4 ± 109.0
12.0	41.2 ± 34.3	61.3 ± 41.2	68.5 ± 40.1
16.0	18.2 ± 15.9	44.3 ± 50.0	38.9 ± 14.2
20.0	17.0 ± 11.2	23.3 ± 36.4	33.3 ± 55.2
24.0	5.7 ± 3.5	22.9 ± 29.9	30.9 ± 45.1
30.0	3.8 ± 1.3	12.0 ± 21.2	7.1 ± 6.5

The tested models assumed that the kinetic processes of absorption, elimination, metabolism follow first-order kinetics. In this initial series of kinetic models (M1-M4) developed solely using data related to QUE alone (Reference group), the hypotheses tested were the presence or absence of lag time and the distribution of QUE, either mono- or bicompartmental, as detailed in Table 3.

Table 3. Characteristics and tested hypotheses of kinetic models for quetiapine (QUE) used in compartmental analysis

Model number	Lag time	Absorption process kinetic order	Number of compartments for QUE distribution
M1	No	1st Order	1
M2	Yes		1
M3	No		2
M4	Yes		2

In this case, model M2, where QUE exhibited lag time during absorption into the bloodstream from the digestive system and followed a mono-compartmental distribution, yielded the lowest AIC value, as shown in Figure 1. Therefore, it was selected for the next modeling step. The one-compartment model assumes that the body functions as a single, uniform compartment, where the drug is distributed instantly and evenly throughout.

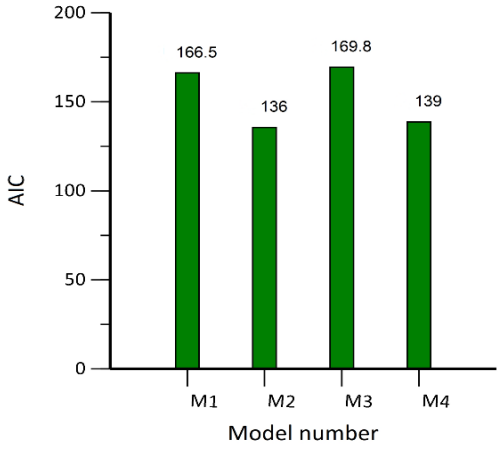

Figure 1. AIC values for kinetic models M1-M4 describing the disposition of quetiapine after a single 85 mg/kg oral dose

In the second step of kinetic modeling, the objective was to identify the most suitable kinetic model for the metabolite NQ while simultaneously integrating the characteristics of QUE disposition (systemic exposure of the drug) determined in the first step. Hypotheses tested included the number of compartments for NQ distribution and its presystemic formation. The characteristics and hypotheses for the NQ models (M21, M22, M23, M24) are detailed in Table 4.

Table 4. Characteristics and tested hypotheses of kinetic models for quetiapine and norquetiapine applied in the second step of compartmental analysis

Model number	Number of compartments for NQ distribution	Presystemic formation of NQ	Systemic metabolism	Other elimination routes for QUE from central compartment
M21	1	No	Yes	Yes
M22	1	Yes	Yes	Yes
M23	2	No	Yes	Yes
M24	2	Yes	Yes	Yes

By incorporating presystemic metabolism into model M22, as opposed to its absence in model M21, the AIC decreased by 30% for the dataset associated with the Reference group. Figure 2 presents the AIC values for the kinetic models tested for the metabolite, highlighting M22 as the most suitable model when including NQ data. This model accounts for the presence of presystemic metabolism in the formation of NQ and its monocompartmental distribution.

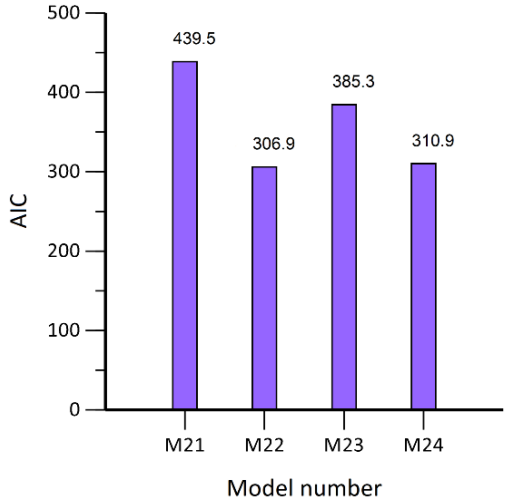

Figure 2. AIC values for kinetic models M21-24 describing the disposition of quetiapine, (administered as a single 85 mg/kg oral dose) and its metabolite, norquetiapine

In the third step, the kinetic model for QUE and NQ, developed in the previous two steps using Reference group data, was further refined by incorporating data from the two Test groups representing QUE's interactions with curcumin (Test 1) and curcuminoids/piperine (Test 2). Data from each Test group was modeled separately alongside the Reference data.

Initially, data from the Reference and Test 1 groups were modeled together. Assuming an identical Vd for both groups, we explored the possibility of differing relative bioavailability due to variations in the absorbed amount of QUE. Accordingly, the M221 and M222 models were developed under the assumption of identical Vd, aiming to test the hypothesis that the absorbed amount of QUE, equivalent to its relative bioavailability, varied between the groups, as shown in Table 5. For modeling the interaction between the Reference and Test 2, the characteristics from the previous

kinetic models and the same hypothesis regarding relative bioavailability were applied. The relative bioavailability was expressed as the 'f_{rel}' parameter, displayed in Table 6. The following notations were also used for calculated parameters (see Table 6, Figure 6 and Figure 7): f_1 and f_2 represent the fraction of quetiapine converted into norquetiapine via presystemic metabolism for Reference and Tests, t_{lag} is the absorption lag time, k_{31} and k_{64} are the absorption rate constants of quetiapine for Reference and Tests, k_{12} and k_{45} are the systemic metabolism rate constants from quetiapine to norquetiapine for the Reference and Tests, k_{10} and k_{20} are the non-metabolic elimination rate constants of quetiapine and norquetiapine, for the Reference, and k_{40} and k_{50} are the elimination rate constants of quetiapine and norquetiapine for the Tests.

Table 5. Characteristics and tested hypothesis of kinetic models for quetiapine and norquetiapine in compartmental analysis, in the context of quetiapine's interactions with curcumin and the curcuminoid/piperine mixture

Model number	Number of compartments for QUE and NQ	Presystemic metabolism	Volume of distribution	Relative bioavailability
M221	1	Yes	Same	Same
M222	1	Yes	Same	Different

The lower AIC values for M222, as shown in Figure 3, justify the introduction of f_{rel} as a parameter into the kinetic model for both QUE interactions. These values support the inference that there is a different relative bioavailability of QUE between the Reference group and the two Test groups, indicating a difference in the amount of QUE absorbed across these groups.

Thus, M222 was chosen the optimal kinetic model for fitting the experimental data of QUE and NQ across all three experimental groups indicating: lag time for QUE absorption, NQ presystemic formation, monocompartmental distribution for both QUE and NQ, systemic formation of NQ from QUE, elimination of NQ and QUE from their central compartments, and distinct relative bioavailability between the Reference and both Test groups.

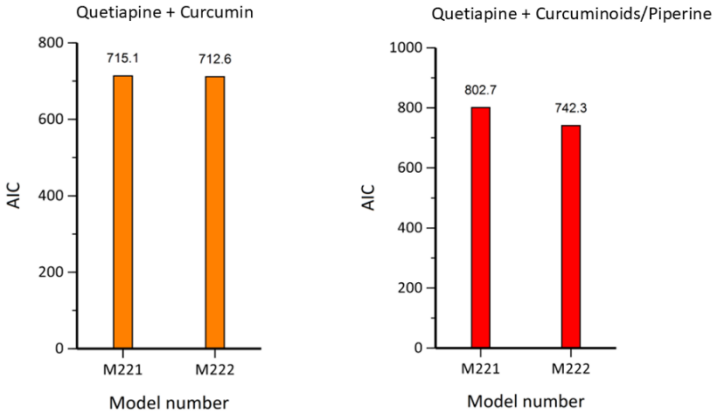

Figure 3. AIC results for compartmental modeling of quetiapine's pharmacokinetic interactions with curcumin (left) and with curcuminoids/piperine (right)

The R-squared values for the observed vs. predicted data of both interactions (Rsq = 0.9861 for Reference and Test 1, and Rsq = 0.9848 for Reference and Test 2), displayed in Figure 4 and Figure 5, respectively, demonstrate the model's predictive accuracy, showing strong agreement between predicted and experimental data.

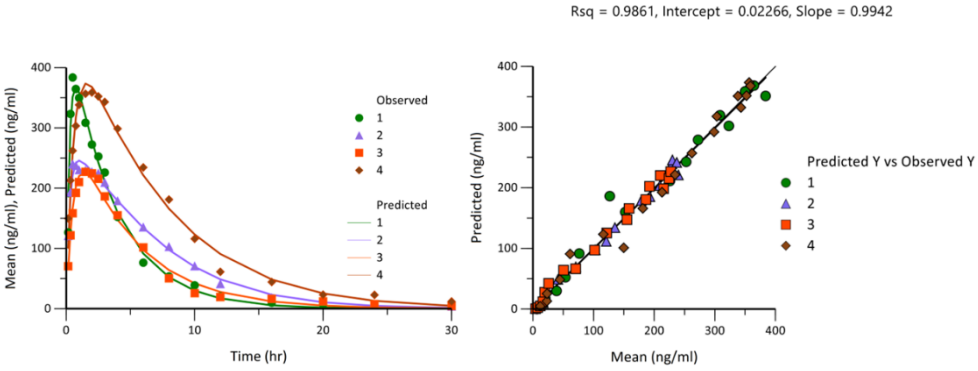

Figure 4. Fitting of M222 for the Reference and Test 1 groups (left) and correlation between experimental data and values predicted by the kinetic model for both groups (right). Legend: quetiapine in the central compartment for the Reference group (1) and Test 1 group (3); norquetiapine in the central compartment for the Reference group (2) and Test 1 group (4)

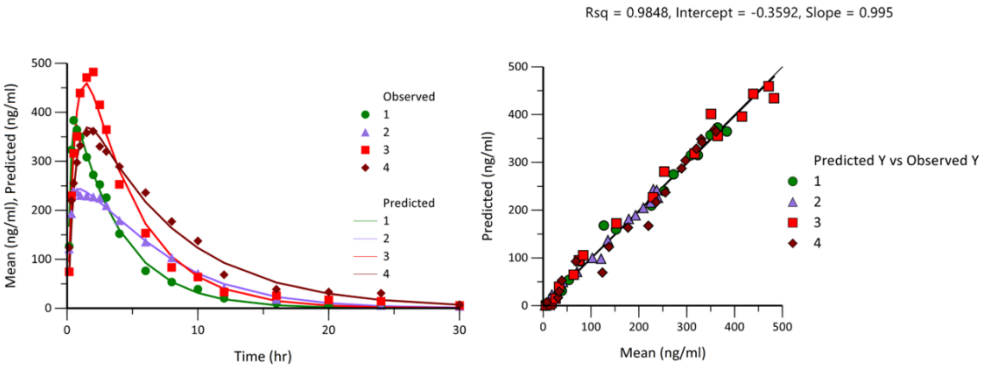

Figure 5. Fitting of M222 for the Reference and Test 2 groups (left) and correlation between experimental data and values predicted by the kinetic model for both groups (right). Legend: quetiapine in the central compartment for the Reference group (1) and Test 2 group (3); norquetiapine in the central compartment for the Reference group (2) and Test 2 group (4)

Table 6. Kinetic parameters of quetiapine and norquetiapine derived from the M222 model in the context of the studied pharmacokinetic interactions

Parameter	U.M.	Estimate for Reference and Test 1	S.E.	Estimate for Reference and Test 2	S.E.
f_1	-	0.4340	0.0125	0.4293	0.0154
f_2	-	0.6628	0.0109	0.4854	0.0106
f_{rel}	-	1.1194	0.0665	1.5967	0.0888
t_{lag}	hr	0.0219	0.0189	0.0663	0.0145
k_{31}	hr^{-1}	3.9700	0.5187	5.2099	0.7758
k_{10}	hr^{-1}	0.1680	0.0838	0.1307	0.0999
k_{12}	hr^{-1}	0.1106	0.0752	0.1408	0.0909
k_{20}	hr^{-1}	0.2105	0.0532	0.2234	0.0654
k_{64}	hr^{-1}	1.8379	0.2064	1.7535	0.1554
k_{40}	hr^{-1}	0.0887	0.2088	0.2434	0.0754
k_{45}	hr^{-1}	0.1200	0.1981	0.0016	0.0676
k_{50}	hr^{-1}	0.1823	0.0681	0.1423	0.0426
Vd	L	106.8405	4.0245	110.0745	4.5440

Modeling the processes underlying drug disposition is a key aspect of pharmacokinetics. Previous studies have employed a one-compartment kinetic model with first-order absorption and elimination for modeling QUE's disposition [11,12]. For instance, in a study involving healthy male adults, plasma QUE concentration–time profiles for immediate-release tablets were effectively

described by a one-compartment distribution model with first-order elimination, supplemented by four transit compartments with first-order transition rate constants to account for delayed absorption [13]. This aspect reinforces the appropriateness of selecting the models which employ a one-compartment distribution (M2 and M22), over M4 or M24, which incorporate a bicompartmental distribution (see Figures 1 and 2). Although the AIC values for the one-compartment models were lower—albeit closely comparable—this further supports their suitability for describing the data.

Comparing the Reference and Test 1 groups, the f_1 and f_2 parameters indicate enhanced presystemic formation of NQ or increased presystemic metabolism of QUE to NQ during Test 1 (43.40% vs. 66.28%). Additionally, k_{64}, the absorption rate constant for QUE during Test 1, was reduced to less than half compared to the reference group (k_{64} = 1.8379 hr^{-1} vs. k_{31} = 3.9700 hr^{-1}). These findings suggest a presystemic interaction mechanism at the intestinal level. Given curcumin's low bioavailability in the absence of absorption enhancers or specialized formulations that increase its systemic availability, these interactions are likely localized at the intestinal presystemic phase. This is further supported by the fact that k_{12} and k_{45} (rate constants for QUE-to-NQ metabolism) remained unchanged between the two study groups, indicating that the systemic metabolism rate was unaffected by the coadministration of QUE and crude curcumin. This minimizes the likelihood of systemic-level interaction involving metabolic enzymes. Furthermore, the f_{rel} parameter reveals a 12% increase in the relative bioavailability of QUE for Test 1. While a lower absorption rate constant (k_a) reflects a less efficient absorption process, an extended duration of absorption may ultimately result in an increased total extent of absorption.

The M222 kinetic model successfully integrated the experimental data for the interaction between QUE and curcuminoids combined with piperine. Similarly, the schematic representation of kinetic processes in Figure 6 (right side) applies to both Test groups. In this case, the relative bioavailability of QUE in Test 2 was 59.6% higher than in the Reference group (f_{rel} = 1.596). The inhibition of hepatic metabolic enzymes, particularly CYP3A4, could explain the increased systemic presence of QUE. The marked reduction in k_{45} compared to k_{12} (0.0016 h^{-1} vs. 0.1408 h^{-1}) supports this hypothesis, suggesting that systemic metabolism might have been inhibited by curcuminoids, potentially with additional contribution from piperine. Furthermore, the reduction in k_{50} compared to k_{20} (0.1423 h^{-1} vs. 0.2234 h^{-1}) suggests that the elimination, specifically the metabolism of NQ, may have also been inhibited by curcuminoids and piperine.

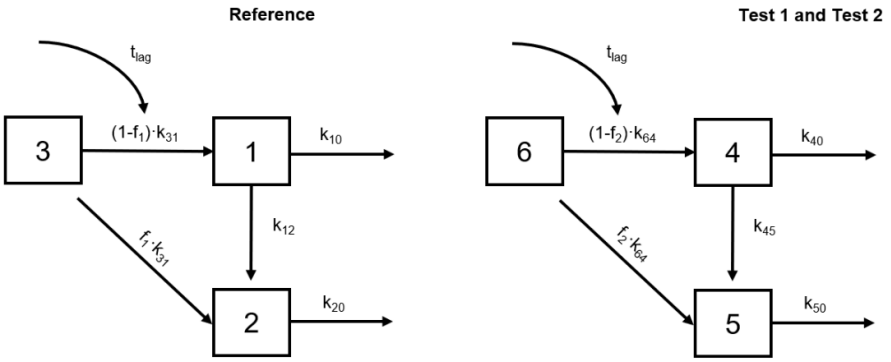

Figure 6. Schematic representation of kinetic processes in the M222 model. On the left is displayed the flowchart for the Reference group. On the right is shown the flowchart for both Test groups; Compartments: "3" and "6" are extravascular absorption sites, "1" and "2" are central compartments for quetiapine and norquetiapine in the Reference group, "4" and "5" are central compartments in the Tests groups

The kinetic models are described by partial differential equations that quantify changes in QUE and NQ concentrations and amounts within each compartment, capturing the processes of absorption, metabolism, and elimination.

$$M222 \begin{cases} \frac{\partial Q_{Qabs3}}{\partial t} = -k_{31} \times Q_{Qabs3} \\ \frac{\partial Q_{Qc1}}{\partial t} = k_{31} \times (1-f_1) \times Q_{Qabs3} - k_{10} \times Q_{Qc1} - k_{12} \times Q_{Qc1} \\ \frac{\partial Q_{Nc2}}{\partial t} = k_{31} \times f_1 \times Q_{Qabs3} \times 0.77 + k_{12} \times Q_{Qc1} \times 0.77 - k_{20} \times Q_{Nc2} \\ \frac{\partial Q_{Qabs6}}{\partial t} = -k_{64} \times Q_{Qabs6} \\ \frac{\partial Q_{Qc4}}{\partial t} = k_{64} \times (1-f_2) \times Q_{Qabs6} - k_{40} \times Q_{Qc4} - k_{45} \times Q_{Qc4} \\ \frac{\partial Q_{Nc5}}{\partial t} = k_{64} \times f_2 \times Q_{Qabs6} \times 0.77 + k_{45} \times Q_{Qc4} \times 0.77 - k_{50} \times Q_{Nc5} \end{cases}$$

Figure 7. Mathematical equations for the M222 kinetic model. Q_{Qabs3} and Q_{Qabs6} represent the amount of quetiapine remaining at the absorption sites for Reference and Test groups, respectively. Q_{Qc1} and Q_{Qc6} denote the amount of quetiapine, while Q_{Nc2}, Q_{Nc5} correspond to the amount of norquetiapine in the central compartments for Reference and Test groups. A molar ratio of 0.77 between quetiapine and norquetiapine was applied to convert moles to mass units from metabolic processes.

The rate constants determined previously (Table 6) provide the mathematical foundation for the equations depicted in Figure 7, enabling the time-dependent modeling of QUE and NQ kinetics across compartments. The metabolic conversion from QUE to NQ occurs on a molar basis, while the equations in Figure 7 use mass units. The molar ratio of 0.77 bridges difference, reflecting their molecular weight ratio.

Data for QUE with curcumin and QUE with curcuminoids/piperine resulted in a lower AIC value for the M222 model. The estimated kinetic parameters, together with their standard error (S.E.), for this model are noted in Table 6, while the flowchart in Figure 6 provides the schematic presentation of the model. Additionally, Figure 7 presents the equations that quantify the temporal changes in QUE and NQ amounts within the model's compartments.

CONCLUSIONS

A three-tier kinetic modeling approach was successfully developed to deepen the understanding of QUE disposition during concomitant administration with curcumin or a curcuminoid/piperine mixture found in food supplements. The distribution of both QUE and its active metabolite, NQ, was best described by a one-compartment model with first-order absorption, metabolism and elimination processes. Enhanced presystemic metabolism of QUE to NQ was observed when curcumin was administered alongside QUE. Varying relative bioavailability was determined between the reference group and each of the two test groups. Systemic metabolism of QUE was markedly influenced by curcuminoids and piperine, while the interaction with curcumin was attributed to a presystemic intestinal mechanism. These findings provide valuable insights into the PK interactions of QUE with herbal supplements, offering a foundation for optimizing therapeutic strategies. While specific dose adjustments for QUE cannot yet be recommended when co-administered with curcumin or curcuminoid derivatives, healthcare providers should remain vigilant about potential PK interactions between this antipsychotic and herbal extracts.

EXPERIMENTAL SECTION

Chemicals and reagents. Quetiapine fumarate substance was sourced from Menadiona (Barcelona, Spain). The norquetiapine analytical standard (97.0% purity), haloperidol pharmaceutical primary standard, methanol analytical reagent, and 98% formic acid were procured from Merck (Darmstadt, Germany). Crude curcumin (97% purity) was sourced from Apollo Scientific (Whitefield, UK),

while the curcuminoids and piperine mixture were taken from Curcumin C3 Complex® + piperine (95% curcuminoids, 380 mg, and 5% piperine, 20 mg/capsule) supplied by Herbagetica (Brașov, Romania).

Study design. The preclinical study protocol was approved by the local ethics committee and the Sanitary and Veterinary Directorate in compliance with the applicable regulations (approval number 322/02.08.2022). Experiments were conducted on healthy adult male Wistar albino rats (10-14 weeks old, 300 ± 50 g) under standard laboratory conditions: temperature (21-25°C), humidity (50 ± 30%) and ventilated cages. Housing spaces were cleaned daily and maintained with 12-hour light-dark cycles and noise reduction. Rats were fed a standard pellet diet and had *ad libitum* access to tap water. The *in vivo* experiment involved three groups of 13 healthy male Wistar albino rats: one reference group and two test groups. The reference group received a single oral dose of QUE (85 mg/kg body weight (b.w.)). The first test group was pretreated with daily oral doses of crude curcumin (200 mg/kg b.w.) for 6 days, followed by a single dose of QUE (85 mg/kg b.w.) administered 30 minutes after the last curcumin dose. The second test group received a 6-day pretreatment with an oral curcuminoid/piperine mixture, followed by a single oral dose of QUE (85 mg/kg). QUE fumarate was dissolved in a 3:1:1 (V/V/V) mixture of water, propylene glycol (cosolvent) and lactic acid (for pH adjustment). Curcumin powder and the curcuminoid/piperine mixture, were suspended in 1% carboxymethylcellulose and vortex-mixed for 5 minutes before each administration.

Sample collection and preparation. A total of 18 blood samples (100 µL each) per rat were collected from the femoral vein into heparinized Eppendorf tubes at intervals starting from 10 minutes to 30 hours after single-dose QUE administration. Blood collection was performed using the BASi Culex ABC® Automatic Blood Collector (BASi, Indiana, USA), which necessitates prior vein cannulation surgery under anesthesia. Samples were stored at -20 °C until analysis. Plasma proteins were precipitated by adding 300 µL of methanol to 100 µL blood. The mixtures were vortexed for 10 seconds (IKA Vortex 2, 1000 rpm) and centrifuged at 10.000 rpm (Sigma 3-30KS centrifuge, 9168× *g*) for 5 minutes. Supernatants were transferred to autosampler vials subsequently analyzed using a HPLC system.

Quantitative determination. Plasma concentrations of QUE and NQ were simultaneously measured using a validated LC-MS/MS method, developed in-house [14] and previously adapted for the quantitation of aripiprazole and dehydroaripiprazole [15]. Chromatographic separation was achieved using an Agilent 1100 series system equipped with a binary pump, autosampler, thermostat and a Zorbax SB-C18 column (100 x 3.0 mm, 3.5 µm) (Agilent Technologies, Santa Clara, CA, USA). Haloperidol, spiked into the blood samples,

served as the internal standard. The mobile phase consisted of 0.3% (m/v) formic acid (eluent A) and acetonitrile (eluent B), eluted in a linear gradient: starting with 10% acetonitrile, increasing to 33% acetonitrile over 3.5 minutes, maintained at 33% until 4.1 minutes, and then re-equilibrated to 10% acetonitrile for 2 minutes. The injection volume was 3 µL, with a flow rate of 1 mL/min and the column temperature set at 40°C. Detection was conducted using a Bruker Ion Trap SL (Bruker Daltonics GmbH, Bremen, Germany) in multiple reaction monitoring mode, with ESI-MS spectra recorded in positive ion mode. Quantification involved the transitions m/z 253 from m/z 384 for QUE, m/z 253 from m/z 296 for NQ and m/z 165 from m/z 376 for haloperidol. Retention times were 3.0 minutes for NQ and 3.3 minutes for QUE. Calibration curves were linear over the 5–1000 ng/mL range, with correlation coefficients (r) of 0.9950 ± 0.0011 for QUE and 0.9935 ± 0.0014 for NQ (mean ± S.D., n = 5).

Data analysis. Kinetic modeling was performed using Phoenix Win Nonlin 8.4 software (Pharsight Company, Mountain View, CA, USA).

The average measured concentration vs. time data for QUE and NQ presented in Table 1 and Table 2 were used to evaluate the disposition parameters of these drugs in the context of their interactions with curcumin derivatives.

A three-tier kinetic modeling approach was conducted to avoid giving rise to excessive number of potential model combinations, which would have rendered the analysis inefficient. To ultimately model QUE and its metabolite, NQ, within the context of their interactions with curcumin and curcuminoids/ piperine, intermediate filtering steps were applied. Initially, kinetic models were developed solely for data related to QUE, deliberately omitting its metabolite and the influence of concomitantly administered substances which may interact with QUE disposition. This step provided a foundational framework for integrating additional data and variables in subsequent steps. The hypotheses tested during this initial step focused on the presence or absence of lag time for QUE absorption and its mono- or bicompartmental distribution, as detailed in Table 3. On the next step, the selected kinetic model for QUE was expanded to identify the optimal model for NQ, for its presystemic formation and distribution type (mono- or bicompartmental), as described in Table 4 alongside additional model characteristics. Finally, the best characteristics previously identified, along with testing the hypothesis of different relative bioavailability between the Reference and Test groups (as outlined in Table 5), were used to develop the final kinetic model that best describes the plasma levels of QUE and NQ across the Reference and the two Test groups.

The Akaike Information Criterion (AIC) was employed as the primary method for discrimination between competing models, enabling the determination of the kinetic model that best fit the experimental data. The AIC is a statistical

tool used to quantify the information content of parameter estimates by relating the weighted sum of squares of residuals (WRSS) to the number of parameters used in the model. When comparing two models with differing parameter counts under the same weighting scheme, AIC imposes a penalty on models with more parameters. The penalty ensures that the more complex model must achieve a sufficiently lower WRSS to justify its added complexity. The model deemed most appropriate is the one with the smallest AIC value [16]. The calculation of AIC was performed using Phoenix WinNonlin 8.4 software (Pharsight Company, Mountain View, CA, USA) with the following formula:

$$AIC = m \times \ln(WSSR) + 2 \times p,$$

where *m* is the number of observations, *WSSR* is the weighted sum of squares of residuals and *p* represents the number of estimated parameters included in the model.

Some assumptions were made to simplify the complex interactions between drug molecules and body systems into a set of solvable equations. The one-compartment model with first-order absorption is based on three fundamental assumptions regarding ADME processes: first-order absorption, instantaneous distribution, and first-order elimination kinetics.

All PK models are derived by formulating the governing mass balance equations and solving them mathematically. Their general form can be expressed as:

$$\frac{\partial(Amount\ of\ Drug)}{\partial t} = [Rate\ of\ Drug\ In] - [Rate\ of\ Drug\ Out]$$

The left side of the equation represents the rate of change in the amount of drug in each compartment, while the right side expresses the net difference between the rates of drug molecules entering and leaving the compartment. For multi-compartment models, a distinct mass balance equation is constructed for each compartment, capturing the specific dynamics of drug movement across the system [9].

ACKNOWLEDGMENTS

This work was supported by an internal research grant offered by “Iuliu Haţieganu” University of Medicine and Pharmacy, Cluj-Napoca, Romania. Research Project no. 882/17/12.01.2022.

REFERENCES

1. Maan JS, Ershadi M, Khan I, et al. Quetiapine. [Updated 2023 Aug 28]. In: StatPearls [Internet]. Treasure Island (FL): StatPearls Publishing; **2024** Jan-. Available online: https://www.ncbi.nlm.nih.gov/books/NBK459145/ (accessed on 12 Feb 2024).
2. DeVane, C.L.; Nemeroff, C.B. Clinical pharmacokinetics of quetiapine: an atypical antipsychotic. *Clin Pharmacokinet* **2001**, *40*, 509-522, doi:10.2165/00003088-200140070-00003.
3. Mauri, M.C.; Paletta, S.; Di Pace, C.; Reggiori, A.; Cirnigliaro, G.; Valli, I.; Altamura, A.C. Clinical Pharmacokinetics of Atypical Antipsychotics: An Update. *Clinical Pharmacokinetics* **2018**, *57*, 1493-1528, doi:10.1007/s40262-018-0664-3
4. Bakken, G.V.; Molden, E.; Hermann, M. Impact of genetic variability in CYP2D6, CYP3A5, and ABCB1 on serum concentrations of quetiapine and N-desalkylquetiapine in psychiatric patients. *Ther Drug Monit* **2015**, *37*, 256-261, doi:10.1097/ftd.0000000000000135.
5. López-Muñoz, F.; Alamo, C. Active metabolites as antidepressant drugs: the role of norquetiapine in the mechanism of action of quetiapine in the treatment of mood disorders. *Front Psychiatry* **2013**, *4*, 102, doi:10.3389/fpsyt.2013.00102.
6. Goswami, S.; Saxena, S.; Yadav, S.; Goswami, D.; Brahmachari, K.; Karmakar, S.; Pramanik, B.; Brahmachari, S. Review of Curcumin and Its Different Formulations: Pharmacokinetics, Pharmacodynamics and Pharmacokinetic-Pharmacodynamic Interactions. *OBM Integrative and Complementary Medicine* **2022**, *07*, 057, doi:10.21926/obm.icm.2204057.
7. Shamsi, S.; Tran, H.; Tan, R.S.J.; Tan, Z.J.; Lim, L.Y. Curcumin, Piperine, and Capsaicin: A Comparative Study of Spice-Mediated Inhibition of Human Cytochrome P450 Isozyme Activities. *Drug Metabolism and Disposition* **2017**, *45*, 49-55, doi:10.1124/dmd.116.073213.
8. Kucukgoncu, S.; Guloksuz, S.; Tek, C. Effects of Curcumin on Cognitive Functioning and Inflammatory State in Schizophrenia: A Double-Blind, Placebo-Controlled Pilot Trial. *J Clin Psychopharmacol* **2019**, *39*, 182-184, doi:10.1097/jcp.0000000000001012.
9. Byers, J.P.; Sarver, J.G. Chapter 10 - Pharmacokinetic Modeling. In *Pharmacology*, Hacker, M., Messer, W., Bachmann, K., Eds.; Academic Press: San Diego, 2009; pp. 201-277.
10. Ahmad, A.M. Recent advances in pharmacokinetic modeling. *Biopharmaceutics & Drug Disposition* **2007**, *28*, 135-143, doi:https://doi.org/10.1002/bdd.540.
11. Methaneethorn, J. Factors Influencing Quetiapine Pharmacokinetic Variability: A Review of Population Pharmacokinetics. *Current Psychiatry Research and Reviews Formerly: Current Psychiatry Reviews* **2024**, *20*, 94-105.
12. Elkomy, M.H. Changing the Drug Delivery System: Does it Add to Non-Compliance Ramifications Control? A Simulation Study on the Pharmacokinetics and Pharmacodynamics of Atypical Antipsychotic Drug. *Pharmaceutics* **2020**, *12*, doi:10.3390/pharmaceutics12040297.

13. Shilbayeh, S.A.; Sy, S.K.; Melhem, M.; Zmeili, R.; Derendorf, H. Quantitation of the impact of CYP3A5 A6986G polymorphism on quetiapine pharmacokinetics by simulation of target attainment. *Clin Pharmacol Drug Dev* **2015**, *4*, 387-394, doi:10.1002/cpdd.172.
14. Ciocotișan, I.-M.; Muntean, D.M.; Gherman, L.-M.; Vlase, L. The influence of multiple-dose oxcarbazepine on the metabolism of single-dose quetiapine. In vivo experiment in rats. *Acta Marisiensis - Seria Medica* **2025**, *71*, 53-59, doi:10.2478/amma-2025-0010.
15. Ciocotișan, I.-M.; Muntean, D.M.; Vlase, L. Bupropion Increased More than Five Times the Systemic Exposure to Aripiprazole: An In Vivo Study in Wistar albino Rats. *Metabolites* **2024**, *14*, doi:10.3390/metabo14110588.
16. Gabrielsson, J.; Weiner, D. Pharmacokinetic and pharmacodynamic data analysis: concepts and applications. 3rd ed. Stockholm: Swedish Pharmaceutical Press; **2001**.